Hopping Multiband OFDM Modulation Systems with Space-Time Frequency Diversity : Multicarrier UWB

Jean Pierre P Cances

Hopping Multiband OFDM Modulation Systems with Space-Time Frequency Diversity : Multicarrier UWB

J. P. CANCES, Xlim/SRI UMR 7252
ENSIL-ENSCI, 16, Rue Atlantis 87068 Limoges cedex, France

Abstract : This paper explores a combination of space-time-frequency (STF) coding and hopping multiband OFDM modulation to build a multiband UWB system. The proposed structure fully exploits all of the spatial and frequency diversities which constitute the main resource advantages of UWB systems. The performance of the proposed multiband UWB system is quantified for Rayleigh and Nakagami-*m* frequency-selective fading channels. In all the cases, it is demonstrated that the maximum achievable diversity of the proposed system is the product of the number of transmit and receive antennas, the number of multipath components and the number of jointly encoded OFDM blocks. As it is illustrated by simulation results, the most interesting property consists in the fact that the diversity gain does not depend on the fading parameter *m*.

I. Introduction

Ultra-wideband (UWB) communications involves the transmission of short pulses with a relatively large fractional bandwidth [1-2]. More specifically, these pulses possess a -10 dB bandwidth which exceeds 500 MHz or 20% of their center frequency and is typically on the order of one to several gigahertz. The large bandwidth occupancy of UWB signals primarily accounts for both the advantages and drawbacks associated with UWB communication systems [3-4]. For instance, the large bandwidth of UWB signals in conjunction with appropriate spreading techniques [5-6] provides robustness to jamming, as well as a low probability of intercept and detection. These favorable characteristics are offset by the fact that UWB communication systems must coexist with narrowband and wideband systems already operating in dedicated frequency bands. In order to minimize interference to these systems, UWB systems must follow strict regulations [3] which limit the achievable data rates [4]-[7], transmission range and implementation of power control. Usually UWB technology uses a single band approach since the sent data are directly transformed into a sequence of impulse waveforms which occupy the available bandwidth of 7.5 GHz.. However, recently, multiband UWB schemes have been proposed [8] for the future IEEE 802.15 standards. These schemes propose to divide the UWB frequency band into several subbands, each with a bandwidth of at least 500 MHz in compliance with the FCC regulations. In order to coherently combine energy from the different multipath components OFDM modulation is planned to modulate the information in each subband. Therefore, the major difference between multiband OFDM and traditional OFDM is that in multiband OFDM the transmitted symbols are not sent on the same frequency band they are interleaved in both time and frequency using all the available subbands.

On the other hand, Multiple-antenna transmission has attracted considerable attention as a means to achieve high bandwidth efficiency and/or high power efficiency over fading channels. Whereas very high data rates are accomplished by multiple antennas both at the transmitter and at the receiver opening equivalent parallel transmission channels, improved reliability of communication is due to increased transmit and/or receive diversity. In case of frequency-non-selective channels space-time (ST) codes have been proposed to exploit the inherent spatial diversity. For frequency selective channels, space-frequency (SF) coded MIMO-OFDM systems is the classical answer since OFDM enables to convert the large band channel into a set of parallel non selective channels. Recently, Giannakis *& al* proposed Space-Time Frequency (STF) codes to exploit all the available diversity in MIMO-OFDM systems.

For UWB systems, the data rates range from 55 Mbits/s to 480 Mbits/s over distances up to ten meters. To enhance the data rates, MIMO systems are now currently envisaged. To this date, MIMO systems have only been planned for the traditional single-band UWB system. Research for MIMO multiband UWB is still at the beginning and constitutes an open area for future research activities.

In our contribution we propose a general study to characterize the performances of UWB-MIMO systems with multiband OFDM. The available spatial and frequency diversities are exploited by the combination of STF coding and hopping multiband UWB transmission. We propose a mathematical model based on the PEP computation for both the cases of Rayleigh and Nakagami fading channels. The case of frequency channels with a wide range of varying multipath components average power and delay is included. The obtained mathematical model quantifies the diversity and the coding gains clearly demonstrating the performance improvements obtained from STF codes and simulation results corroborate the theoretical analysis.

The paper is organized as follows: in section II the multiband UWB-MIMO system model is presented together with the channel model and the receiver structure with the detection algorithm. In section III, a performance analysis of a peer-to-peer multiband UWB-MIMO is given. Simulation results are given in section IV while section V contains the conclusion.

II. System Model

We deal with a multiband OFDM scenario that has been already proposed in the IEEE 802.15.3a WPAN standard. The available UWB spectrum of 7.5 GHz is divided into several subbands. Each subband has a bandwidth BW of at least 500 MHz. Each user needs one subband per transmission, and for each user signals from all transmit antennas share the same subband. Within each subband, OFDM modulation with N subcarriers is used at each transmit antenna. Various modulation and channel coding schemes together with different frequency spreading or time spreading rates can be applied yielding to variable bit rates. We study a multiband system with fast band-hopping rate: the signal is transmitted on a given subband during one OFDM symbol interval and then transmitted on a different subband for the next OFDM symbol interval.

1. *Transmitter architecture*

We consider a peer-to-peer multiband UWB system with N_t transmit and N_r receive antennas, as shown in Fig. 1. The information is encoded across N_t transmit antennas, N OFDM subcarriers and K OFDM blocks.

At the transmitter, the coded information sequence from a channel encoder is partitioned into blocks of N_b bits. Each block is mapped onto a $KN \times N_t$ STF codeword matrix.

$$\boldsymbol{D} = [\boldsymbol{D}_0^T \ \boldsymbol{D}_1^T \cdots \boldsymbol{D}_{K-1}^T]^T \qquad (1)$$

where

$$\boldsymbol{D}_k = [\boldsymbol{d}_1^k \ \boldsymbol{d}_2^k \cdots \boldsymbol{d}_{N_t}^k] \text{ and } \boldsymbol{d}_i^k = [d_i^k(0)\ d_i^k(1) \cdots d_i^k(N-1)]^T \text{ for } i = 1,2,\cdots,N_t \text{ and } k = 0,1,\cdots,K-1$$

The symbol $d_i^k(n)$, n = 0,1,…,N-1, represents the complex symbol to be transmitted over subcarrier n by transmit antenna i during the k^{th} OFDM symbol period. The matrix $\boldsymbol{D}$ is normalized to have average energy $E\left[\|\boldsymbol{D}\|^2\right] = K.N.N_t$, where $\|.\|$ denotes the Frobenius norm. At the k^{th} OFDM block, the transmitter applies N-point IFFT over each column of the matrix $\boldsymbol{D}_k$, yielding an OFDM symbol of length T_{FFT}.

The IFFT output is added with a cyclic prefix of length T_{CP} and a guard interval of duration T_{GI}, and then passed through a digital-to-analog converter, resulting in an analog baseband OFDM signal of duration $T_{SYM}=T_{FFT}+T_{CP}+T_{GI}$. The baseband OFDM signal to be transmitted by the i^{th} transmit antenna at the k^{th} OFDM block can be expressed as:

$$x_i^k(t) = \sqrt{\frac{E}{N_t}}.\sum_{n=0}^{N-1} d_i^k(n).\exp\left\{\left(j.2.\pi.n.\Delta f\right)\left(t-T_{CP}\right)\right\} \qquad (2)$$

for $t \in \left[T_{CP}, T_{FFT}+T_{CP}\right]$ and with $\Delta f = 1/T_{FFT} = BW/N$ which represents the frequency separation between two adjacent subcarriers. The complex baseband signal $x_i^k(t)$ is filtered, up-converted to an RF signal with a carrier frequency f_c^k and sent from the i^{th} transmit antenna. Thus, the multiband UWB signal at the i^{th} transmit antenna can be written:

$$s_i(t) = \sum_{k=0}^{K-1} \mathrm{Re}\left\{x_i^k\left(t-k.T_{SYM}\right).\exp(j.2.\pi.f_c^k.t)\right\} \qquad (3)$$

The carrier frequency f_c^k specifies the subband, in which the signal is transmitted during the k^{th} OFDM symbol period. The carrier frequency is changed from one OFDM block to another, so as to enable frequency diversity together with multiple access interference mitigation. Frequency f_c^k remains the same for every transmit antenna, and the transmissions from all of the N_t transmit antennas are simultaneous and synchronous. Considering that N_b information bits are transmitted in $K.T_{SYM}$ seconds, the transmission rate without taking into account the channel encoder is $R = N_b/(K.T_{SYM})$.

2. *Channel model*

We consider frequency-selective fading channels; they are modeled as tapped-delay line with L taps. At the k^{th} OFDM block, the channel impulse response from the i^{th} transmit to the j^{th} receive antenna can be described as :

$$h_{ij}^k(t) = \sum_{l=0}^{L-1} \alpha_{ij}^k(l).\delta(t-\tau_l) \qquad (4)$$

$\alpha_{ij}^k(l)$ is the multipath gain coefficient, L denotes the number of resolvable paths, and τ_l represents the path delay of the l^{th} path. Experimental measurements in UWB indoor environments indicate that the amplitude of each multipath component is good approximated by a log-normal or Nakagami-*m* distribution. The advantage of Nakagami-*m* distributions is that they can model a wide range of fading conditions by adjusting their fading parameters. In

fact, Nakagami-*m* distributions with large value *m* are similar to the log-normal distributions. Therefore, we will assume that the amplitude of the l^{th} path, $\left|\alpha_{ij}^{k}(l)\right|$, is modeled as a Nakagami-*m* random variable with fading parameter *m* and average power $\Omega_l = E\left[\left|\alpha_{i,j}^{k}(l)\right|^2\right]$. The powers of the *L* paths are normalized such that $\sum_{l=0}^{L-1}\Omega_l = 1$. We assume that the time delay τ_l and the average power Ω_l are the same for every transmit-receive antenna pair.

3. *Receiver Processing*

The signal at each receive antenna is a superposition of N_t transmitted signals corrupted by additive white Gaussian noise (AWGN). Assuming a perfect synchronization at the receiver, the received RF signal at each receive antenna is down-converted to a complex baseband signal, matched to the pulse waveform, and then sampled before passing through an OFDM demodulator. After the OFDM demodulator discards the cyclic prefix and performs an N-point FFT, a maximum-likelihood detection is performed across all the N_r receive antennas. The choice of a cyclic prefix length greater than the duration of the channel impulse response ensures that no interblock interference (IBI) between OFDM words is present. In fact, OFDM enables to decouple the frequency selective fading channel into a set of *N* parallel frequency-non-selective fading channels, whose fading coefficients are equal to the channel frequency response at the center frequency of the subcarriers. The received signal at the n^{th} subcarrier at receive antenna *j* during OFDM block *k* can be expressed as:

$$y_j^k(n) = \sqrt{\frac{E}{N_t}}\sum_{i=1}^{N_t} d_i^k(n).H_{ij}^k(n) + z_j^k(n) \qquad (5)$$

with

$$H_{ij}^k(n) = \sum_{l=0}^{L-1}\alpha_{ij}^k(l).\exp\left[-j.2.\pi.\Delta f.\tau_l\right] \qquad (6)$$

which represents the frequency response of the channel at subcarrier *n* between the i^{th} transmit and the j^{th} receive antenna during the k^{th} OFDM word. In (5), $z_j^k(n)$ represents the noise sample, which is modeled as complex Gaussian random variable with zero mean and a two-sided power spectral density of $N_0/2$.

Equation (5) can be written in matrix form when considering the complete set of subcarriers as given below:

$$\boldsymbol{Y}_j = \sqrt{\frac{E}{N_t}}.\boldsymbol{S}_D.\boldsymbol{H}_j + \boldsymbol{Z}_j \qquad (7)$$

where $\boldsymbol{S}_D$ is a $K.N \times K.N.N_t$ data matrix: $\boldsymbol{S}_D = [\boldsymbol{S}_1 \ \boldsymbol{S}_2 \cdots \boldsymbol{S}_{N_t}]$. $\boldsymbol{S}_i$ is a $K.N \times K.N$ diagonal matrix whose main diagonal comprises the information data from transmit antenna *i*. $\boldsymbol{S}_i$ is written as: $\boldsymbol{S}_i = diag\left(\left[(\boldsymbol{d}_i^0)^T \ (\boldsymbol{d}_i^1)^T \cdots (\boldsymbol{d}_i^{K-1})^T\right]^T\right)$. The $K.N.N_t \times 1$ channel vector $\boldsymbol{H}_j$ is of a form $\boldsymbol{H}_j = \left[\boldsymbol{H}_{1j}^T \ \boldsymbol{H}_{2j}^T \cdots \boldsymbol{H}_{N_t j}^T\right]^T$ with $\boldsymbol{H}_{ij} = \left[H_{ij}^0(0) \cdots H_{ij}^0(N-1) \cdots H_{ij}^{K-1}(0) \cdots H_{ij}^{K-1}(N-1)\right]^T$. The received signal vector $\boldsymbol{Y}_j$ of size $K.N.N_r \times 1$ is given by :

$$\boldsymbol{Y}_j = diag\left(\left[(\boldsymbol{y}_j^0)^T \ (\boldsymbol{y}_j^1)^T \cdots (\boldsymbol{y}_j^{K-1})^T\right]^T\right)$$

in which $\boldsymbol{y}_j^k$ is an $N \times 1$ vector whose n^{th} element is $y_j^k(n)$. The noise vector $\boldsymbol{Z}$ has the same form as $\boldsymbol{Y}$ by replacing $y_j^k(n)$ with $z_j^k(n)$. We assume that the receiver has perfect knowledge of the channel state information, but the transmitter doesn't get it. The receiver exploits a maximum likelihood decoder, where the decoding process is jointly performed on N_r receive signal vectors. The decision rule can be stated as :

$$\hat{\boldsymbol{D}} = \arg\min_{\boldsymbol{D}} \sum_{j=1}^{N_r} \left\| \boldsymbol{Y}_j - \sqrt{\frac{E}{N_t}}.\boldsymbol{S}_D.\boldsymbol{H}_j \right\|^2 \qquad (8)$$

III. Performance Analysis

In this section we derive the theoretical performances of the proposed multiband UWB scheme. We build our analysis on the derivation of the pairwise error probability (PEP). We define first $\Delta_S = \boldsymbol{S}_D - \boldsymbol{S}_{\hat{D}}$ which represents the difference between two data matrices $\boldsymbol{S}_D$ and

$\boldsymbol{S}_{\hat{D}}$. The computation steps of the PEP is the same as those given in [15], the PEP for a given channel realization is given by :

$$P_{e|\boldsymbol{H}_j} = Q\left(\sqrt{\frac{\rho}{2.Nt}.\sum_{j=1}^{N_r}\left\|\Delta_S \boldsymbol{H}_j\right\|^2}\right) \qquad (9)$$

with $\rho = E/N_0$ which represents the average signal-to-noise ratio (SNR) at each receive antenna and $Q(x)$ is the Gaussian error function: $Q(x) = \frac{1}{\sqrt{2.\pi}}.\int_x^{+\infty} \exp(-\frac{s^2}{2}).ds$. The average PEP can be obtained by calculating the expected value of the conditional PEP with respect to the distribution of $\gamma = \sum_{j=1}^{N_r}\left\|\Delta_S \boldsymbol{H}_j\right\|^2$:

$$P_e = \int_0^{+\infty} Q\left(\sqrt{\frac{\rho}{2.N_t}.s}\right).p_\gamma(s).ds \qquad (10)$$

$p_\gamma(s)$ is the probability density function (PDF) of γ. Henceforth, the main difficulty consists in the derivation of the distribution law of $\gamma = \sum_{j=1}^{N_r}\left\|\Delta_S \boldsymbol{H}_j\right\|^2$. To do this we look for a more convenient expression of γ in matrix form. We introduce at first the $N_t.N_r.L.K \times 1$ channel vector : $\boldsymbol{a} = \left[\boldsymbol{a}_1^T, \boldsymbol{a}_2^T, \cdots, \boldsymbol{a}_{N_r}^T\right]^T$, where $\boldsymbol{a}_j$ contains the multipath gains from all transmit antennas to the j^{th} receive antenna. The $N_t.L.K \times 1$ vector $\boldsymbol{a}_j$ is written as :

$$\boldsymbol{a}_j = \left[\left(\boldsymbol{a}_{1j}^0\right)^T \cdots \left(\boldsymbol{a}_{N_t j}^0\right)^T \cdots \left(\boldsymbol{a}_{1j}^{K-1}\right)^T \cdots \left(\boldsymbol{a}_{N_t j}^{K-1}\right)^T\right]^T \qquad (11)$$

in which : $\boldsymbol{a}_{ij}^k = \left[\alpha_{ij}^k(0)\ \alpha_{ij}^k(1) \cdots \alpha_{ij}^k(L-1)\right]^T$.

Using the definition of (6) and (11), we can express $\boldsymbol{H}_j = \left[\boldsymbol{H}_{1j}^T\ \boldsymbol{H}_{2j}^T \cdots \boldsymbol{H}_{N_t j}^T\right]^T$ as :

$$\boldsymbol{H}_j = \left(\boldsymbol{I}_{K.N_t} \otimes \boldsymbol{W}\right)\boldsymbol{a}_j$$

where $\otimes$ denotes the Kronecker product, $\boldsymbol{I}_M$ represents the $M \times M$ identity matrix, and $\boldsymbol{W}$ is an $N \times L$ Fourier matrix transform whose $(n,l)^{th}$ component is $\exp(-j.2.\pi.\Delta f.\tau_l)$. We can then rewrite γ as :

$$\gamma = \sum_{j=1}^{N_r} \left\| \Delta_S (\boldsymbol{I}_{KN_t} \otimes \boldsymbol{W}) \boldsymbol{a}_j \right\|^2 \qquad (12)$$

It is easily seen from (12) that the distribution of γ depends on the joint distribution of the multipath gain coefficients $\alpha_{ij}^k(l)$. Using (12) we are now ready to derive P_e, we will consider at first the case of mutiband UWB-MIMO systems with independent fading. In this context we can completely characterize the diversity and the coding gains. Then, we investigate the case of a more realistic system with correlated fadings.

1. *Independent fading*

Due to the frequency hopping, the K OFDM symbols in each STF codeword are transmitted over different subbands. With an ideal band hopping, we assume that the signal transmitted over K different subbands undergo independent fading. We also suppose that the path gains $\alpha_{ij}^k(l)$ are independent for different paths and different transmit-receive links, and each transmit-receive link has the same power delay profile, i.e., $E\left[\left| \alpha_{ij}^k(l) \right|^2 \right] = \Omega_l$. Using this the autocorrelation matrix of $\boldsymbol{a}_j$ is given by :

$$E\left[\boldsymbol{a}_j . \boldsymbol{a}_j^H \right] = \boldsymbol{I}_{KN_t} \otimes \boldsymbol{\Omega} \qquad (13)$$

We have: $\boldsymbol{\Omega} = diag(\Omega_0, \Omega_1, \cdots, \Omega_{L-1})_{L \times L}$ which contains all the power delay profile of the L paths. Denote $\boldsymbol{\Omega}^{1/2} = diag(\sqrt{\Omega_0}, \sqrt{\Omega_1}, \cdots, \sqrt{\Omega_{L-1}})_{L \times L}$ and define $\boldsymbol{q}_j$ as $\boldsymbol{q}_j = \left(\boldsymbol{I}_{KN_t} \otimes \boldsymbol{\Omega}^{1/2} \right)^{-1} \boldsymbol{a}^j$, it is straightforward to demonstrate that the elements of $\boldsymbol{q}_j$ are identically independent distributed (iid) Nakagami-m random variables with normalized power $\Omega = 1$. Substitute $\boldsymbol{a}_j = \left(\boldsymbol{I}_{K.N_t} \otimes \boldsymbol{\Omega}^{1/2} \right) \boldsymbol{q}_j$ into (12), and apply the property of Kronecker product we obtain

:

$$\gamma = \sum_{j=1}^{N_r} \left\| \Delta_S \left(\boldsymbol{I}_{K.N_t} \otimes \boldsymbol{W}\boldsymbol{\Omega}^{1/2} \right) \boldsymbol{q}_j \right\|^2 = \sum_{j=1}^{N_r} \boldsymbol{q}_j^H \boldsymbol{\psi}\, \boldsymbol{q}_j \qquad (14)$$

where $\boldsymbol{\psi} = (\boldsymbol{I}_{K.N_t} \otimes \boldsymbol{W}\boldsymbol{\Omega}^{1/2})^H . \Delta_S^H . \Delta_S . (\boldsymbol{I}_{K.N_t} \otimes \boldsymbol{W}\boldsymbol{\Omega}^{1/2})$. Since $\boldsymbol{\psi}$ is a Hermitian matrix of size $K.N_t.L \times K.N_t.L$, it can be decomposed into $\boldsymbol{\psi} = \boldsymbol{V}.\boldsymbol{\Lambda}.\boldsymbol{V}^H$, where $\boldsymbol{V} = \left[\mathbf{v}_1 \cdots \mathbf{v}_{K.N_t.L} \right]$ is a unitary matrix whose diagonal elements are the eigenvalues of $\boldsymbol{\psi}$. After some manipulations, we arrive at :

$$\gamma = \sum_{j=1}^{N_r} \sum_{n=1}^{K.N_t.L} \lambda_n(\boldsymbol{\psi}) \left| \beta_{j,n} \right|^2 \qquad (15)$$

with $\beta_{j,n} = \mathbf{v}_n^H \boldsymbol{q}_j$. Since $\boldsymbol{V}$ is unitary and components of $\boldsymbol{q}_j$ are iid, $\beta_{j,n}$'s are independent random variables, whose magnitudes are approximately Nakagami-$\tilde{m}$ distributed with :

$$\tilde{m} = \left(K.L.N_t.m \right) / (K.L.N_t.m - m + 1) \qquad (16)$$

and average power $\Omega = 1$. Hence, the pdf of $\left| \beta_{j,n} \right|^2$ approximately follows Gamma distribution. Now, to obtain the average PEP, we have to substitute (15) into (9), and averaging (9) with respect to the distribution of $\left| \beta_{j,n} \right|^2$. To do this we use an alternate representation of the *Q* function, $Q(x) = \frac{1}{\pi} \int_0^{\pi/2} \exp\left(-\frac{x^2}{2.\sin^2\theta}\right) . d\theta$ for $x \geq 0$. We are now able to express (9) in terms of moment generating function (MGF) of γ, denoted by $\phi_\gamma(s)$. Using $\phi_{\left|\beta_{j,n}\right|^2}(s) = \left(1 - \frac{\Omega}{\tilde{m}} . s \right)^{-\tilde{m}}$ and the fact that the $\left| \beta_{j,n} \right|^2$ are independent, the average PEP is given by :

$$P_e = \frac{1}{\pi} \int_0^{\pi/2} \prod_{n=1}^{K.L.N_t} \left(1 + \frac{\rho\left(\Omega / \tilde{m}\right)}{4.Nt.\sin^2\theta} . \lambda_n(\boldsymbol{\psi}) \right)^{-\tilde{m}.N_r} . d\theta \qquad (17)$$

By bounding the PEP above with $\theta = \pi / 2$ and assuming high SNR, we obtain the following upper bound for the PEP :

$$P_e \le \left[\prod_{n=1}^{rank(\boldsymbol{\psi})} \left(\frac{\rho}{4N_t} . \frac{\Omega}{\tilde{m}} . \lambda_n(\boldsymbol{\psi}) \right) \right]^{-\tilde{m}.N_r} \qquad (18)$$

$\left\{ \lambda_n(\boldsymbol{\psi}) \right\}_{n=1}^{rank(\boldsymbol{\psi})}$ are nonzero eigenvalues of matrix $\boldsymbol{\psi}$. From (18), we can quantify the performance of STF coded multiband UWB with the diversity gain $G_d = \min_{\boldsymbol{D} \ne \hat{\boldsymbol{D}}} \tilde{m}.Nr.rank(\boldsymbol{\psi})$, and the coding gain $G_c = \min_{\boldsymbol{D} \ne \hat{\boldsymbol{D}}} \frac{\Omega}{\tilde{m}} . \left(\prod_{n=1}^{rank(\boldsymbol{\psi})} \lambda_n(\boldsymbol{\psi}) \right)^{1/rank(\boldsymbol{\psi})}$.

In order to specify the maximum achievable diversity gain, we calculate the rank of $\boldsymbol{\psi}$ as follows. According to (14) and the rank property, we have $rank(\boldsymbol{\psi}) = rank(\Delta_S(\boldsymbol{I}_{K.N_t} \otimes \boldsymbol{W}\boldsymbol{\Omega}^{1/2}))$. Observe that the size of Δ_S is $K.N \times K.N.N_t$, whereas the size of $\boldsymbol{W}\boldsymbol{\Omega}^{1/2}$ is $N \times L$. Therefore, the rank of matrix $\boldsymbol{\psi}$ becomes $rank(\boldsymbol{\psi}) \le \min\left\{ K.N, KL.N_t \right\}$ and the maximum achievable diversity gain is :

$$G_d^{\max} = \min\left\{ \tilde{m}.K.L.N_t.N_r, \tilde{m}.K.N_r.N \right\} \qquad (19)$$

Note that the diversity gain in (19) depends on the parameter $\tilde{m}$ which is close to one for any fading parameter *m*. Indeed, for multiband UWB-MIMO systems,

$$\tilde{m} = \left(1 - (K.L.N_t)^{-1} + (K.L.N_t.m)^{-1} \right)^{-1} \approx 1 \qquad (20)$$

In this case, the maximum achievable diversity gain is well approximated by :

$$G_d^{\max} = \min\left\{ K.L.N_t.N_r, K.N_r.N \right\} \qquad (21)$$

The result in the analysis just given above is somewhat surprising since the diversity gain of multiband UWB-MIMO system does not depend on the fading parameter *m*. This can be justified with the following argument: since $\beta_{j,n}$ in (15) is a normalized sum of $K.L.N_t$ independent Nakagami random variables, when $K.L.N_t$ is large enough, $\beta_{j,n}$ behaves like a complex Gaussian random variable, and hence the channel is quite similar to a Rayleigh fading one. For a classical ultra-wideband environment there are always a large number of

multipath components and so the effect of $K.L.N_t$ on the diversity gain dominates the effect of fading parameter *m*. This implies that the diversity advantage does not depend on the severity of the fading. The diversity gain obtained under Nakagami fading with arbitrary *m* parameter is almost the same as that obtained in Rayleigh fading channels.

We have to insist here on the major difference between the use of STF coding in the conventional OFDM systems and in the multiband OFDM systems. For STF coding in the conventional OFDM systems, the symbols are continuously transmitted in the same subband, hence the temporal diversity depends only on the time vrying nature of the propagation channel. In contrast, the diversity gain in (21) reveals that with band switching, the STF coded multiband UWB is able to achieve the diversity gain of $\min\left\{K.L.N_t.N_r, K.N.N_r\right\}$ regardless of the channel time-correlation property.

Another important point is that ST and SF coded UWB systems are included in the general proposed PEP derivation. In the case of single-carrier frequency-non-selective channel, i.e. $N = 1$ and $L = 1$, the performance of STF coded UWB is similar to that of ST coded UWB system. In case of coding with one OFDM block ($K = 1$), the performance of STF coded UWB is the same as that of SF coded scheme. The maximum diversity reduces to $\min\left\{L.N_t.N_r, N.N_r\right\}$. This reveals that STF coding together with band hopping across *K* OFDM blocks can offer the diversity advantage of *K* times larger than that of SF coding approach.

2. *Correlated fading*

In case of correlated fading, we express γ in (12) as :

$$\gamma = \boldsymbol{a}^H \left\{ \boldsymbol{I}_{N_r} \otimes \left[\left(\boldsymbol{I}_{K.N_t} \otimes \boldsymbol{W}^H \right) \Delta_S^H \Delta_S \left(\boldsymbol{I}_{K.N_t} \otimes \boldsymbol{W} \right) \right] \right\} \boldsymbol{a} \qquad (22)$$

To simplify the analysis, we assume that the channel correlation matrix, $\boldsymbol{R}_A = E\left[\boldsymbol{a}.\boldsymbol{a}^H\right]$ is of full rank. Since $\boldsymbol{R}_A$ is positive definite Hermitian symmetric, it has a symmetric square root $\boldsymbol{U}$ such that $\boldsymbol{R} = \boldsymbol{U}^H \boldsymbol{U}$, where $\boldsymbol{U}$ is also of full rank. Let define $\boldsymbol{q} = \boldsymbol{U}^{-1}\boldsymbol{a}$, then it follows that $E\left[\boldsymbol{q}.\boldsymbol{q}^H\right] = \boldsymbol{I}_{KLN_tN_r}$ i.e. the components of $\boldsymbol{q}$ are uncorrelated. Substituting $\boldsymbol{a} = \boldsymbol{U}\boldsymbol{q}$ into (22), we have $\gamma = \boldsymbol{q}^H \boldsymbol{\Phi} \boldsymbol{q}$ where

$$\boldsymbol{\Phi} = \boldsymbol{U}^H \left\{ \boldsymbol{I}_{N_r} \otimes \left[\left(\boldsymbol{I}_{K.N_t} \otimes \boldsymbol{W}^H \right) \Delta_S^H \Delta_S \left(\boldsymbol{I}_{K.N_t} \otimes \boldsymbol{W} \right) \right] \right\} \boldsymbol{U} \qquad (23)$$

Accordingly, using an eigenvalue decomposition of the matrix $\boldsymbol{\Phi}$, we can express γ as $\gamma = \sum_{n=1}^{KLN_tN_r} \lambda_n(\boldsymbol{\Phi}) \left| \beta_n \right|^2$ where $\beta_n = \mathbf{v}_n^H . \boldsymbol{q}$, $\mathbf{v}_n$'s and $\lambda_n(\boldsymbol{\Phi})'s$ are the eigenvectors and the eigenvalues of matrix $\boldsymbol{\Phi}$. From (11), the PEP can be obtained by averaging the conditional PEP with respect to the joint distribution of $\left\{ \left| \beta_n \right|^2 \right\}$:

$$P_e = \int_0^\infty \cdots \int_0^\infty Q\left(\sqrt{\frac{\rho}{2.N_t} . \sum_{n=1}^{M} \lambda_n(\boldsymbol{\Phi})\, s_n} \right) \times p_{|\beta_1|^2 \cdots |\beta_M|^2}(s_1, \cdots, s_M)\, ds_1 \cdots ds_M \qquad (24)$$

where $M = KLN_tN_r$. In general, $\beta_n's$ for different *n* are not independent, and the closed-form solution for (24) is difficult, if not possible, to determine. In what follows, we will discuss two special cases where (24) can be further simplified.

Special case 1: constant fading

In case of constant fading over *K* OFDM blocks, i.e., the modulated OFDM signal is transmitted continously over the same subband for entire *K* OFDM blocks, (12) can be re-expressed as :

$$\gamma = \sum_{j=1}^{N_r} \left\| \left(\boldsymbol{C}_D - \boldsymbol{C}_{\hat{D}} \right) (\boldsymbol{I}_{N_t} \otimes \boldsymbol{W}) \tilde{\boldsymbol{a}}_j \right\|^2 \qquad (25)$$

where $\boldsymbol{C}_D = [\boldsymbol{C}_0^T \boldsymbol{C}_1^T \cdots \boldsymbol{C}_{K-1}^T]^T$ is a $KN \times N_t N$ matrix, and $\boldsymbol{C}_k = \left[diag\left(\boldsymbol{d}_1^k \right) \cdots diag\left(\boldsymbol{d}_{N_t}^k \right) \right]$. The channel vector $\tilde{\boldsymbol{a}}_j$ of size $L.N_t \times 1$ is given by $\tilde{\boldsymbol{a}}_j = \left[\boldsymbol{a}_{1j}^T \boldsymbol{a}_{2j}^T \cdots \boldsymbol{a}_{N_t j}^T \right]^T$ in which $\boldsymbol{a}_{ij}^k = \left[\alpha_{ij}^k(0)\, \alpha_{ij}^k(1) \cdots \alpha_{ij}^k(L-1) \right]^T$. Due to the fact that the path gains $\boldsymbol{a}_{ij}^k's$ are the same for every *k*, $0 \le k \le K-1$, the time superscript index *k* is omitted to simplify the notations. Following the previous steps, we can show that the average PEP has the same form as (24) with *M* replaced by $L.N_t.N_r$ and $\left\{ \lambda_n(\tilde{\boldsymbol{\Phi}}) \right\}_{n=1}^{LN_tN_r}$ being the eigenvalues of :

$$\tilde{\boldsymbol{\Phi}} = \tilde{\boldsymbol{U}}^H \left\{ \boldsymbol{I}_{N_r} \otimes \left[\left(\boldsymbol{I}_{N_t} \otimes \boldsymbol{W}^H \right) \Delta_C^H \Delta_C \left(\boldsymbol{I}_{N_t} \otimes \boldsymbol{W} \right) \right] \right\} \tilde{\boldsymbol{U}} \qquad (26)$$

Here, we have $\Delta_C = \boldsymbol{C}_D - \boldsymbol{C}_{\hat{D}}$ and $\tilde{\boldsymbol{U}}$ is a symmetric square root of $\tilde{\boldsymbol{R}}_A = E\left[\tilde{\boldsymbol{a}}.\tilde{\boldsymbol{a}}^H \right]$, in which $\tilde{\boldsymbol{a}} = \left[\tilde{\boldsymbol{a}}_1^T \; \tilde{\boldsymbol{a}}_2^T \cdots \tilde{\boldsymbol{a}}_{N_r}^T \right]^T$. Assuming further that the path gains are independent for every transmit-receive link, the average PEP can be obtained similarly as in Section III-1 as :

$$P_e \le \left[\prod_{n=1}^{rank(\boldsymbol{\Theta})} \left(\frac{\rho}{4N_t} . \frac{\Omega}{\tilde{m}} . \lambda_n(\boldsymbol{\Theta}) \right) \right]^{-\tilde{m}.N_r} \qquad (27)$$

where $\lambda_n(\boldsymbol{\Theta})$ are the nonzero eigenvalues of the matrix $\boldsymbol{\Theta} = \left(\boldsymbol{I}_{N_t} \otimes \boldsymbol{W}^H \right) \Delta_C^H \Delta_C \left(\boldsymbol{I}_{N_t} \otimes \boldsymbol{W} \right)$. One can observe that the minimum rank of $\Delta_C \left(\boldsymbol{I}_{N_t} \otimes \boldsymbol{W} \right)$ is $\min\left\{ LN_t, KN \right\}$. Hence, the maximum achievable diversity gain becomes :

$$G_d^{\max} = \min\left\{ \tilde{m}LN_t N_r, \tilde{m}KNN_r \right\} \qquad (28)$$

Since KN is typically larger than LN_t, we can conclude from (28) that when K OFDM symbols are sent on one subband prior to band switching, coding across K OFDM blocks does not offer any additional diversity advantage compared to the coding scheme within one OFDM block.

Special case 2: fading parameter $m = 1$.

With $m = 1$, Nakagami is equivalent to Rayleigh distribution, and the path gain coefficients can be modeled as complex Gaussian random variables. Recall that for Gaussian random variables, uncorrelated implies independent. Thus, $\left\{ \left| \beta_n \right|^2 \right\}$ in (24) becomes a set of iid Rayleigh random variables. By the use of MGF of γ, the average PEP in (24) is given by :

$$P_e = \frac{1}{\pi} \int_0^{\pi/2} \prod_{n=1}^{K.L.N_t.N_r} \left(1 + \frac{\rho}{4.Nt.\sin^2\theta} . \lambda_n(\boldsymbol{\Phi}) \right)^{-1} . d\theta \qquad (29)$$

where $\boldsymbol{\Phi}$ is defined in (23). The PEP can be bounded by :

$$P_e \leq \left[\prod_{n=1}^{KLN_t N_r} \left(\frac{\rho}{4.N_t} \lambda_n(\boldsymbol{\Phi}) \right) \right]^{-1} \qquad (30)$$

at high SNR. Therefore, the performance of this system can be quantified as the diversity gain: $G_d = \min_{\boldsymbol{D} \neq \hat{\boldsymbol{D}}} N_r.rank(\boldsymbol{\Phi})$, and the coding gain: $G_d = \min_{\boldsymbol{D} \neq \hat{\boldsymbol{D}}} N_r.rank(\boldsymbol{\Phi})$, and the coding gain: $G_c = \min_{\boldsymbol{D} \neq \hat{\boldsymbol{D}}} \left(\prod_{n=1}^{rank(\boldsymbol{\Phi})} \lambda_n(\boldsymbol{\Phi}) \right)^{\frac{1}{rank(\boldsymbol{\Phi})}}$.

IV. **Simulation Results**

We performed simulations for multi-antenna multiband UWB systems with N = 256 subcarriers and the subband bandwidth of BW = 500 MHz. The OFDM symbol is of duration $T_{FFT} = 256/500.10^6 = 512\,ns$. After adding the cyclic prefix of length $T_{CP} = 62\,ns$ and the guard interval of length 10 ns, the symbol duration becomes $T_{SYM} = 512 + 62 + 10 = 584\,ns$. In this contribution, as channel model, we utilize the same channel model that has been worked out by the IEEE 802.15SG3a research group. This model is inspired by the Markovian Saleh/Valenzuela channel model: the multi-path components scattered from the same impulse are grouped in cluster, at the receiver side. Each cluster is composed by some rays, i.e. by some pulses. The clusters arrival time is modelled as a Poisson process with rate Λ while the rays arrival time is characterized by a rate λ. In the S/V model, the gain of each ray is a complex random variable whose phase can uniformly vary in the interval [-π, π]. The path amplitudes $\left|\alpha_{ij}^k(l)\right|$ follow a Nakagami-*m* distribution. The power delay profile, used to specify the path delays τ_l'*s* and powers Ω_l'*s* follows the statistical model in IEEE 802.15SG3a. STF codes have been recently extensively studied; a very promising approach has been proposed by W. Su *& al* . They deal with the problem of systematic SF block code design for MIMO-OFDM systems and they propose an SF code design approach that offers full symbol rate and guarantees full diversity for an arbitrary number of transmit antennas, any modulation scheme and arbitrary power delay profiles while maintaining low computational decoding complexity. In our simulations, the STF codeword $\boldsymbol{D} = [\boldsymbol{D}_0^T \; \boldsymbol{D}_1^T \cdots \boldsymbol{D}_{K-1}^T]^T$ in (1) is further simplified as:

$$\boldsymbol{D}_k = \left[\boldsymbol{G}_{k,1}^T \boldsymbol{G}_{k,2}^T \cdots \boldsymbol{G}_{k,P}^T \ \ \mathbf{0}_{(N-P\gamma N_t)\times N_t}^T \right]$$

in which γ is a fixed integer between 1 and L, $P = \lfloor N/(\gamma.N_t) \rfloor$, and $\mathbf{0}_{m\times n}$ stands for an $m \times n$ all-zeros matrix. The $\gamma N_t \times N_t$ code matrices $\{\boldsymbol{G}_{k,p}\}_{k=0}^{K-1}$ for each p are jointly designed, whereas the matrices $\boldsymbol{G}_{k,p}$ and $\boldsymbol{G}_{k',p'}$ with $p \neq p'$ are designed independently. For example, with the simple example of two transmit antennas we propose the STF repetition code, $\boldsymbol{G}_{k,p}$ given by :

$$\boldsymbol{G}_{k,p} = \left(\boldsymbol{I}_{N_t} \otimes \mathbf{1}_{\gamma\times 1} \right) \begin{pmatrix} x_{p,1} & x_{p,2} \\ -x_{p,2}^* & x_{p,1}^* \end{pmatrix} \qquad (31)$$

where $\mathbf{1}_{m\times n}$ denotes an $m \times n$ matrix with all ones, $x_{p,i}$'s belong to a MPSK constellation. In this case, $\boldsymbol{G}_{k,p}$ are the same for all k's. An other possible code is given by the following matrix code:

$$\boldsymbol{G}_{k,p} = \sqrt{N_t} \begin{pmatrix} \boldsymbol{x}_{p,1}^k & \mathbf{0}_{\gamma\times 1} \\ \mathbf{0}_{\gamma\times 1} & \boldsymbol{x}_{p,2}^k \end{pmatrix} \qquad (32)$$

where $\boldsymbol{x}_{p,i}^k$ is a $\gamma \times 1$ matrix constructed as follows. Omitting subscript p and denoting $\zeta = K.\gamma.N_t$, the $1 \times \zeta$ matrix $\boldsymbol{x} = \left[\left(\boldsymbol{x}_1^0\right)^T \left(\boldsymbol{x}_2^0\right)^T \cdots \left(\boldsymbol{x}_1^{K-1}\right)^T \left(\boldsymbol{x}_2^{K-1}\right)^T \right]$ is given by :

$$\boldsymbol{x} = \left(1/\sqrt{K}\right).\boldsymbol{s}.\boldsymbol{V}(\theta_1, \theta_2, \cdots \theta_\zeta) \qquad (33)$$

in which $\boldsymbol{s} = \left[s_1 \, s_2 \cdots s_\zeta \right]$ is a vector of MPSK symbols and $\boldsymbol{V}$ is a Vandermonde matrix with $\theta_l = e^{j(4l-3)\pi/(2.\zeta)}$ for $\zeta = 2^s$ $(s \geq 1)$ and $\theta_l = e^{j(6l-1).\pi/(3.\zeta)}$ with $\zeta = 2^s.3^t$ $(s \geq 0, t \geq 1)$.

At first we study the performance of the proposed coding approach over one OFDM block (K = 1). We use both the simple repetition encoding scheme and full rate codes, each with spectral efficiency of 1 bit/s/Hz (without taking prefix and guard interval into account). The

data rate is of 195 Mbits/s. Fig. 2 displays the performance results of the STF coded UWB system with $\gamma = 2$. We notice that regardless of particular coding scheme, the spatial diversity gained from multi-antenna architecture does improve the system performance significantly. In addition, the performance can be further improved with the choice of STF codes and permutation schemes. In Fig. 3, we compare the performance of multiband UWB system with different frequency diversity orders. Here, we employ the full rate code with γ = 2, 3 and 4. We can see that by increasing the number of jointly encoded subcarriers, the system performance can be improved. This is in complete accordance with the theoretical result in (18). Therefore, with a properly designed STF code, we can effectively exploit both spatial and frequency diversities in UWN environment.

Second, we compare the performances of STF coded multiband UWB system with fast band-hopping rate and time spreading factors, K = 1, 2. Fig. 4 shows the performances of full-rate STF codes with γ = 2 and spectral efficiency of 1 bit/s/Hz. It is apparent that the diversity advantage increases with the number of jointly encoded OFDM blocks. Such achieved improvement results from the band hopping rather than the temporal diversity, and hence the diversity order increases significantly regardless of the temporal correlation of the channel. This enforces the analytical results in Section III.1 that the diversity order of STF coded multiband UWB with fast hopping rate increases with K.

Finally, we compare the performance of multiband systems with different band-hopping rates. Fig. 5 depicts the performance of full rate STF coded UWB system with γ = 2 and K = 2. We observe the performance degradation when the band-hoopping rate decreases, which corresponds to the results in (18) and (27) that coding over multiple OFDM blocks will offer the additional diversity advantage when the STF coding is applied together with fast band-hopping scheme, i.e., the K OFDM symbols in each STF codeword are transmitted on various frequency-bands.

V. **Conclusions**

In this paper, using a technique of band hopping together with coding across spatial, temporal and frequency dimensions, we built a MIMO UWB system which is able to completely exploit all available spatial and multipath diversities which are of crucial importance in UWB environments. We showed that the maximum achievable diversity advantage of our proposed system is the product of four quantities: the number of transmit antennas, the number of

receive antennas, the number of jointly encoded OFDM blocks and the number of multipath components in the channel equivalent model. Simulation results proved that band hopping and STF coding techniques increase considerably the diversity order, and therefore the overall BER system performance. For example, considering a single-antenna system, increasing the number of jointly encoded OFDM blocks from one to two yields an improvement of 6 dB at BER = 10^{-4}. Furthermore, doubling the number of transmit antennas entails an improvement of 9 dB at BER = 10^{-4}.

References

[1] M. Di Benedetto, G. Giancola, "Understanding Ultra Wide Band radio fundamentals", *Prentice Hall*, 2004.

[2] M. Z. Win, R. A. Scholtz, "Ultra-wide bandwidth time hopping spread-spectrum impulse radio for wireless multiple-access communications", *IEEE Trans. Comm.*, vol. 48, April 2000, pp. 679-689.

[3] A. R. Forouzan, M. Nasiri-Kenari, J.A Salehi, "Performance analysis of time-hopping spread-spectrum multiple-access systems: uncoded and coded schemes", *IEEE Trans. Wireless Comm.*, vol. 1, issue 4, Oct. 2002, pp. 671-681.

[4] M. L. Welborn, "System considerations for ultra-wideband wireless networks," in IEEE Radio Wireless Conf., Aug. 2001, pp. 5–8.

[5] J. R. Foerster, "The performance of a direct-sequence spread ultrawideband system in the presence of multipath, narrowband interference, and multiuser interference," in IEEE Conf. Ultra Wideband Systems Tech., May 2002, pp. 87–91.

[6] N. Boubaker and K. B. Letaief, "Ultra wideband DSSS for multiple access communications using antipodal signaling," in IEEE Int. Conf. Commun., vol. 3, May 2003, pp. 11–15.

[7] E. Saberinia and A. H. Tewfik, "Pulsed and nonpulsed OFDM ultra wideband wireless personal area networks," in IEEE Conf. Ultra Wideband Systems Tech., Nov. 2003, pp. 275–279.

[8] J. R. Foerster et al., Intel CFP Presentation for a UWB PHY, Mar. 3, 2003. IEEE P802.15-03/109r1.

.

Figures Caption

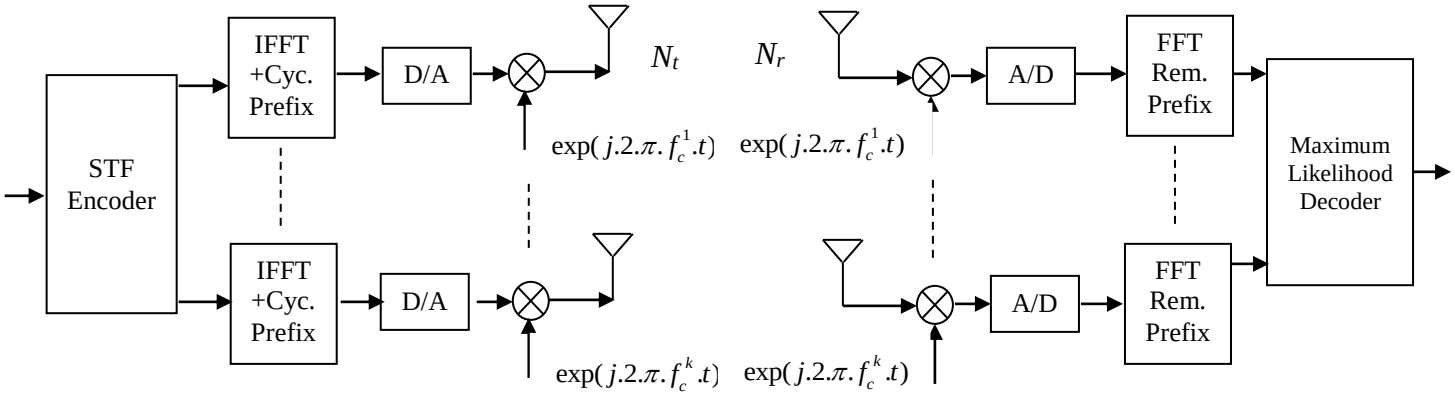

Fig 1 : Multiband UWB-MIMO systems

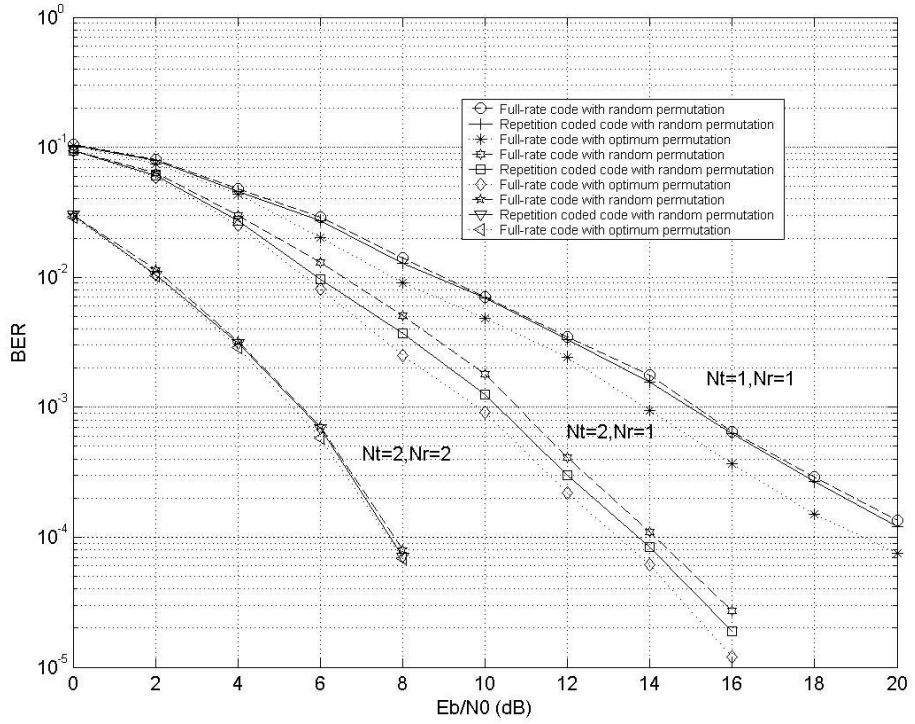

Fig 2 : Performance of multiband UWB-MIMO systems with different codes (K = 1)

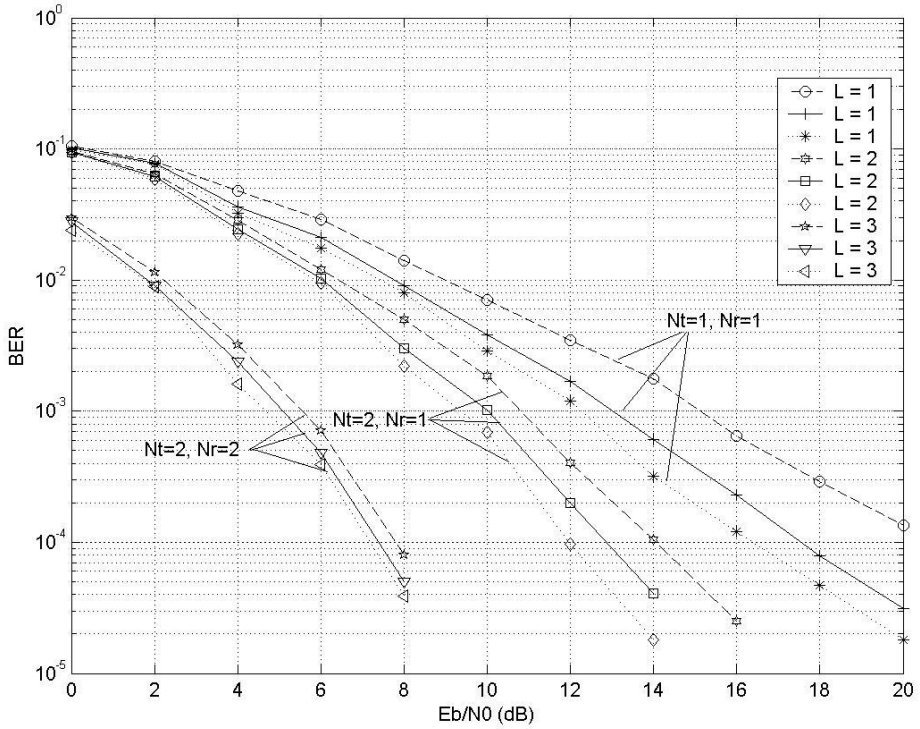

Fig 3 : Performance of multiband UWB with different diversity orders

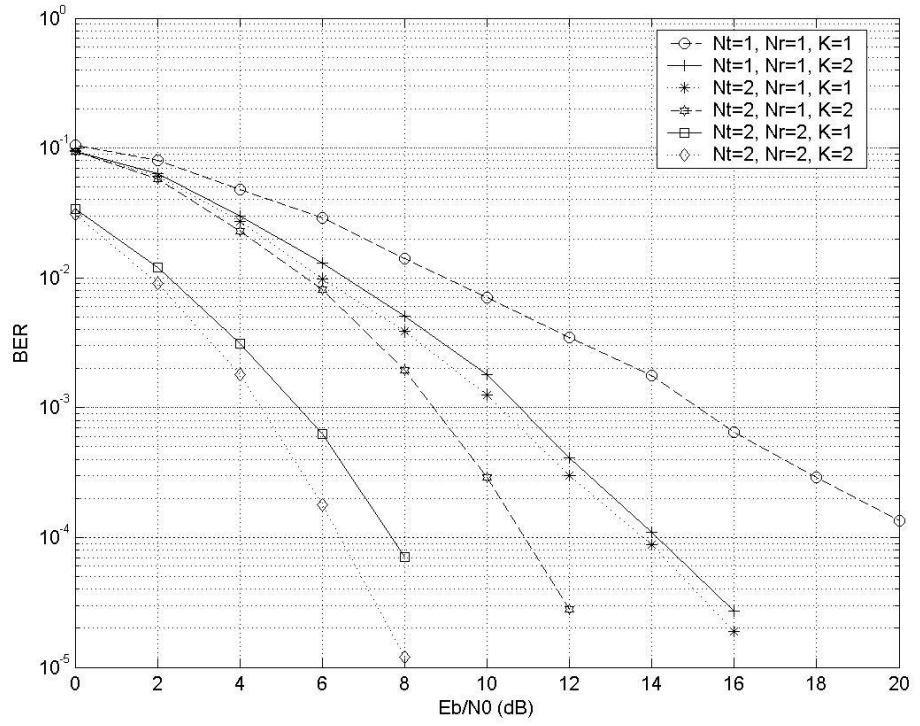

Fig 4 : Performance of multiband UWB-MIMO systems with different time-spreading factors

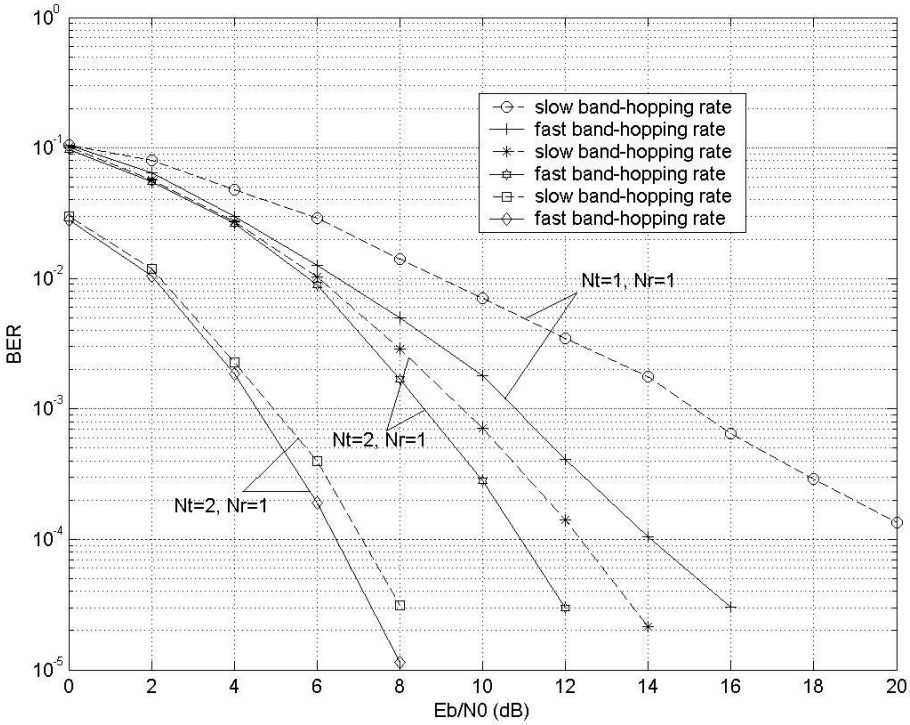

Fig 5 : Performance of multiband UWB-MIMO systems with different hopping rates